Volatile Element Chemistry during Metamorphism of Ordinary Chondritic Material and Some of its Implications for the Composition of Asteroids

By

Laura Schaefer

And

Bruce Fegley, Jr.

Planetary Chemistry Laboratory
Department of Earth and Planetary Sciences
Washington University
St. Louis, MO 63130-4899
laura_s@wustl.edu
bfegley@wustl.edu

Submitted to Icarus

4 January 2008

Revised: March 26 2009
Revised: July 23, 2009

Pages: 55
Tables: 5
Figures: 5

Proposed Running Head: Volatile element metamorphic chemistry on asteroids

Corresponding Author:

Laura Schaefer

Campus Box 1169

Department of Earth and Planetary Science

Washington University

One Brookings Dr.

St. Louis, MO 63130-4899

laura_s@wustl.edu

Phone: 314-935-6310

Fax: 314-935-7361

Abstract:

We used chemical equilibrium calculations to model thermal metamorphism of ordinary chondritic material as a function of temperature, pressure, and trace element abundance and use our results to discuss volatile mobilization during thermal metamorphism of ordinary chondrite parent bodies. We compiled trace element abundances in H, L, and LL chondrites for the elements Ag, As, Au, Bi, Br, Cd, Cs, Cu, Ga, Ge, I, In, Pb, Rb, Sb, Se, Sn, Te, Tl, and Zn, and identified abundance trends as a function of petrographic type within each class. We calculated volatility sequences for the trace elements in ordinary chondritic material, which differ significantly from the solar nebula volatility sequence. Our results are consistent with open system thermal metamorphism. Abundance patterns of Ag and Zn remain difficult to explain.

Keywords: asteroids, metamorphism, geochemistry

1. Introduction

Recently we used chemical equilibrium calculations to model thermal outgassing of ordinary chondritic material as a function of temperature, pressure and bulk composition (Schaefer and Fegley, 2007a). This work considered the chemistry of 20 major, trace, and volatile elements (Al, C, Ca, Cl, Co, Cr, F, Fe, H, K, Mg, Mn, N, Na, Ni, O, P, S, Si, and Ti). We discussed the results relevant to outgassing and atmospheric formation in our earlier paper. However, the chemical equilibrium calculations in Schaefer and Fegley (2007a) also provide the foundation for modeling chemistry of the volatile major and trace elements during thermal metamorphism of ordinary chondritic material. The reason for this is as follows.

During thermal metamorphism, volatile elements may vaporize into the gas phase and be transported in the parent body. The details of this process depend to some extent on the molecular speciation of the elements in the gas phase. In turn, this speciation depends on the fugacities (equal to partial pressures for ideal gases) of more abundant elements such as oxygen, sulfur, hydrogen, nitrogen, chlorine, and fluorine in the gas phase. The chemistry of volatile trace elements (e.g., Pb, Bi, In, Tl, etc.) depends upon that of the major elements, but does not alter major element chemistry because the volatile trace elements are much less abundant than the major elements. However, the chemistry of volatile trace elements with similar abundances may be interconnected.

Our work addresses three important questions. First, do elemental volatilities during ordinary chondrite metamorphism differ from those during condensation in the solar nebula? This question is important because cosmochemists presently use the nebular volatility sequence to discuss metamorphic chemistry of volatile elements. Second, does thermal metamorphism

affect the abundances and chemistry of volatile elements in ordinary chondrites? Third, do volatile element abundances vary inside thermally metamorphosed asteroids?

We focus on moderately and highly volatile trace elements (Ag, As, Au, Bi, Br, Cd, Cs, Cu, Ga, Ge, I, In, Pb, Rb, Sb, Se, Sn, Te, Tl, Zn) in this paper for two reasons. First, thermal metamorphism was isochemical with respect to the major rock-forming elements such as Ca, Mg, Al, Si, Fe, and Ti (McSween et al., 1988). Second, Schaefer and Fegley (2007a) found that the abundances of F, Cl, and S, which are also volatile elements, are unaltered by thermal metamorphism. These elements are mainly in minerals throughout the range of metamorphic temperatures instead of being in the gas phase.

Our paper is organized as follows. Section 2 gives background information on ordinary chondrites and thermal metamorphism. Section 3 discusses the trace element abundances in H-, L-, and LL-chondrites and abundance trends as a function of petrographic type. Section 4 describes our thermodynamic calculations. In Section 5, we discuss the results of our thermodynamic calculations for the trace elements. In Section 6, we describe the calculated volatility sequence and compare it to solar nebula volatility and trace element mobility in ordinary chondrites. We also discuss, using our results, possible mechanisms for producing the observed trends in the trace element abundances. Section 7 gives our answers to the questions posed in the introduction, summarizes our research, and suggests how it can be extended. Schaefer and Fegley (2007b) presented preliminary results of this work.

2. Some Background Information about Ordinary Chondrites

Ordinary chondrites make up about 97% of all chondrites and are the most abundant type of meteorites. They are unmelted stony meteorites that contain metal, silicate, sulfide, and oxide minerals in varying proportions. The ordinary chondrites are divided into three groups (H, L, LL)

on the basis of the total elemental abundance of iron and the abundance of iron metal. The H-chondrites (~49% by number of all ordinary chondrites) have high total iron and high iron metal. The L-chondrites (~36%) have low total iron, and the LL-chondrites (~14%) have low total iron and low iron metal.

As mentioned in our prior paper (Schaefer and Fegley, 2007a), chondrites are samples of material from the solar nebula. Different types of chondritic material (e.g., carbonaceous, ordinary, enstatite) analogous to different types of chondritic meteorites are generally believed to be the building blocks of the Earth and other rocky bodies. Chemical equilibrium calculations, cosmochemical models, and geochemical data indicate that ordinary chondritic material was abundant in the inner solar nebula where the terrestrial planets formed, and many have modeled the Earth as a mixture of chondritic components (e.g., see Barshay, 1981; Hart and Zindler, 1986; Kargel and Lewis, 1993; Larimer, 1971; Lewis and Prinn, 1984; Lodders, 2000; Lodders and Fegley, 1997; Wänke, 1981).

Although they are samples of nebular material, the ordinary chondrites are not unaltered, and underwent dry thermal metamorphism at 400˚ – 1,000˚ C at relatively low pressures (< 2 kilobars) on their parent bodies (McSween et al., 1988). A numerical scale running from 3 to 6 for the H-, L-, and LL-ordinary chondrites denotes the degree of metamorphic alteration. For example, the type 3 (unequilibrated) chondrites with metamorphic temperatures ranging from 400˚ – 600˚ C are the least metamorphically altered while the type 4 – 6 (equilibrated) chondrites with metamorphic temperatures ranging from 600˚ – 1000˚ C are more altered. (The terms equilibrated and unequilibrated refer to the homogeneity of ferromagnesian silicates, but do not imply thermochemical equilibrium or lack thereof.)

The observed variations among unequilibrated chondrites are sufficiently great that they are further sub-divided into types 3.1 – 3.9. The large variations are not surprising because chemical equilibria and chemical reaction rates vary exponentially with temperature, i.e., log K_{eq} or log k_{rate} vs. 1/T (in Kelvins) is linear where K_{eq} is the equilibrium constant and k_{rate} is the rate constant for a chemical reaction. The inverse temperature range (10^4/T = 11.45 – 14.86) across the type 3 chondrites is much greater than across any other petrographic type and is almost as wide as the inverse temperature range across all equilibrated chondrites (10^4/T = 7.85 – 11.45). On this basis, greater variations in chemical composition are expected within the type 3 chondrites than within any other single petrographic type.

The effects of thermal metamorphism on the chemistry of ordinary chondrites have been studied for over 40 years. As noted earlier, these studies show that thermal metamorphism was isochemical with respect to major rock-forming elements. However, thermal metamorphism apparently altered the abundances, distribution with petrographic type, and speciation of *some* volatile trace elements in ordinary chondrites. For example, Otting and Zähringer (1967) showed that the abundances of the noble gases (^{36}Ar, ^{132}Xe) varied inversely with petrographic type. Carbon contents also vary inversely with petrographic type from type 3.1 – 3.9, although the variation is not as clear from types 4 – 6. Tandon and Wasson (1968) showed that the In concentration varied inversely with petrographic type in L-chondrites. Keays et al. (1971) showed strong depletions and abundance variations of Cs, Br, Cd, Bi, Tl, In, ^{36}Ar, ^{132}Xe and C, and showed that the abundances of many of these volatile elements were correlated with one another, in particular ^{132}Xe and In, which also illustrates the decrease of In with petrographic type. More recent evidence from studying the stable isotopic compositions of Zn, Cu, Cd, and Ag in ordinary chondrites shows that they are variable, although variations do not correlate with

abundance or with petrographic type (Luck et al. 2003, 2005; Schönbächler et al. 2008; Wombacher et al. 2003, 2008). However, the variation in isotopic composition may have been caused by open-system thermal metamorphism. In contrast, Wolf and Lipschutz (1998) found no statistically significant abundance trends for several volatile trace elements (Co, Rb, Ag, Se, Te, Zn, Cd, Bi, In) with petrographic type in H4 – H6 chondrites. They did not look at H3 chondrites.

If thermal metamorphism is responsible for elemental abundance variations as a function of petrographic type, it has important implications for elemental abundances on asteroids, which are the meteorite parent bodies. The onion-skin model for meteorite metamorphism on asteroids postulates that the more metamorphosed type 6 – 4 equilibrated chondrites come from the hotter, higher pressure interior of an asteroid and that the less metamorphosed type 3.9 – 3.1 unequilibrated chondrites come from the colder, lower pressure surface regions. Dreibus and Wänke (1980) proposed that volatile elements were transported from the hotter interiors to the cooler outer layers of meteorite parent bodies. Other workers have made similar suggestions. If such ideas are correct, our chemical equilibrium calculations should predict a radial variation of volatile element concentrations and host phases inside asteroidal parent bodies and an enrichment in volatile elements in surficial regions compared to those at the time of parent body formation. These predictions are testable using geochemical analyses conducted by remote sensing and in situ methods. We return to this idea in Section 6 where we compare our calculations with observations.

3. Trace Element Abundances in Ordinary Chondrites

We compiled abundances for 15 moderately volatile (As, Ag, Au, Bi, Cs, Cu, Ga, Ge, Pb, Rb, Sb, Se, Sn, Te, Zn) and 5 highly volatile trace elements (Br, Cd, I, In, and Tl) in H-, L-, and

LL- chondrite falls. We use the conventional definition of the moderately volatile elements as those with 50% condensation temperatures (50% T_c) in the solar nebula greater than FeS (664 K), whereas highly volatile elements have 50% T_c lower than FeS (Lodders et al., 2009). The 50% T_c refers to the temperature at which 50% of the element is condensed. This temperature is independent of the absolute abundance for trace elements (Lodders, 2003). We used the METBASE meteorite database (Koblitz, 2005) and additional references to compile abundances (Binz et al., 1976; Dennison and Lipschutz, 1987; Fehr et al. 2005; Friedrich et al., 2003, 2004; Huston and Lipschutz, 1984; Keays et al., 1971; Lingner et al., 1987; Luck et al., 2005; Neal et al., 1981; Walsh and Lipschutz, 1982; Wang et al., 1999; Wolf and Lipschutz, 1995; Wolf et al., 1997). We used abundance data only for observed meteorite falls, and neglected abundance data for finds, which are subject to terrestrial contamination and leaching. The overall range, means (arithmetic and geometric), and medians for the trace elements in H-, L-, and LL-chondrite falls of all petrographic types are given in Tables 1-3.

Variations of trace element abundances between petrographic types are discussed in Section 3.1 and are shown in Figure 1. We examined the available analyses to determine if the trends previously observed in trace element abundances with petrographic type (Morgan et al., 1985; Sears and Weeks, 1986; Lingner et al., 1987; Keays et al., 1971; Wai and Wasson, 1977) are real or due to limited or biased sample bases (Kallemeyn et al., 1989; Wolf and Lipschutz, 1998). We used only data for chondrite falls because many minor and trace elements are susceptible to leaching (e.g., Rb and Cs, Gast 1962) and contamination (e.g., Pb, Unruh, 1982) in finds. However, not all falls are immune from these problems and not all finds are affected by them. For example, some specimens of the Beardsley H5 chondrite were collected a year or so after it fell and are depleted in alkalis due to weathering. In contrast, the Potter L6 chondrite is a

find with a terrestrial residence time longer than 20,000 years but it is not depleted in K relative to other L-chondrites (Goles, 1971).

We included data for all shock types; however, it has been shown that there are compositional trends with shock type for the L-chondrites (Neal et al., 1981; Walsh and Lipschutz, 1982; Huston and Lipschutz, 1984), with abundances significantly lower in more highly shocked (S4-S6) chondrites, than in mildly shocked (S1-S3) chondrites. A similar trend is not observed for H-chondrites (Lingner et al., 1987). The analyses which we used are split approximately evenly between mildly and highly shocked meteorites.

We calculated mean (both arithmetic and geometric) and median abundances for each trace element in each petrographic type and for each class (H, L, LL) as a whole. (Although we include the H/L3s in Fig. 1, abundances for these chondrites were not used in the calculation of the overall H chondrite abundances given in Table 1.) We found that trends in arithmetic mean abundances with petrographic type, where observed, are typically subtle and can be easily obscured by inclusion of one or two anomalously large or small analyses. Geometric means and medians are generally in better agreement. The geometric mean and the median abundances track trends much better as they are less susceptible than arithmetic means to the effects of outlying data. For instance, the increase of Tl abundances with increasing petrographic type in H4 – H6 chondrites, observed by Wolf and Lipschutz (1998), is only apparent for the arithmetic mean abundances and is less observable for the geometric means. The median Tl abundances are constant throughout the H4 – H6 chondrites.

3.1 Trace Element Abundances Across Petrographic Type

Figure 1 shows the abundances of the trace elements in H-, L- and LL- chondrites, respectively, relative to their abundances in CI chondrites (Lodders 2003). The elements are ordered along the

x-axis in accordance with their 50% T_c in the solar nebula, from least volatile (As) to most volatile (Tl) (Lodders 2003). The 50% T_c are given in Table 4 for reference. The figure shows geometric mean abundances for each of the major petrographic types (3, 4, 5, 6). We use geometric means because they are less skewed by very large and very small outlying analyses. Lines represent the 1σ error on the geometric means. The moderately volatile elements (As through Se) as a whole show much smaller variations in abundance across petrographic type than the highly volatile elements (Cd through Tl). However, there are some exceptions, which we address below.

3.1.1. Moderately Volatile Elements (As, Au, Cu, Ag, Sb, Ga, Ge, Rb, Cs, Bi, Pb, Zn, Te, Sn, Se). As seen in Fig. 1, the abundances of As, Au, Cu, Sb, Ga, Zn, and Se, and – to a slightly lesser extent – Rb, Te, and Ag are relatively constant across petrographic type. Arsenic shows slightly more variation than Au or Cu, but there is no systematic trend with petrographic type. Arsenic abundances differ by at most a factor of 1.5x for H- and L-chondrites, and 1.6x for LL-chondrites. The abundances of As, Au, and Cu decrease slightly from H- to L- to LL-chondrites. This is to be expected since these elements concentrate in the metal phase, which is more abundant in H-chondrites than in L- or LL-chondrites. Copper shows slight stable isotope variations of δ^{65}Cu = -0.5 to +0.1‰, increasing from H- to L- to LL-chondrites (Luck et al. 2003). Correlation of δ^{65}Cu with Δ^{17}O indicates that low temperature metamorphism did not significantly alter the Cu isotopic composition in ordinary chondrites. Luck et al. (2003) suggest that Cu was instead isotopically heterogeneous in the solar nebula.

Antimony is slightly more abundant in L-chondrites than in H- or LL-chondrites and is more variable in the LL-chondrites. However, there are only two analyses for the LL4 chondrites. Disregarding the LL4s, the remaining LL petrographic types are fairly constant. The

abundance of Ga is very constant and is nearly identical for all of the ordinary chondrites. The Se abundances in H- and L-chondrites are essentially constant across petrographic type. The Se abundances in LL3 and LL4 chondrites are ~1.3x larger than those in LL5 and LL6 chondrites. This is very similar to the pattern of Te abundances in LL-chondrites.

Zinc abundances do not show a significant trend with petrographic type, although the L4 chondrites are somewhat high due to 3 large analyses. However, the isotopic composition of zinc δ^{66}Zn varies by ~1 ‰ in ordinary chondrites, increasing from LL- to L- to H-chondrites, and, unlike Cu, is independent of Δ^{17}O (Luck et al. 2005). Luck et al. (2005) suggest that the zinc isotopic composition was affected by parent body metamorphism, which made the H3s and L3s isotopically lighter than the higher petrographic types. While we do not see any evidence that the H3s or L3s were enriched in Zn, Luck et al. (2005) calculate that a δ^{66}Zn shift of 1.6 ‰ would only require a 10% loss of Zn from the higher petrographic types. The measured δ^{66}Zn shift from H3 to H6 is only ~ 0.4‰, so the abundance change would be smaller than 10%, which may not be noticeable in our mean abundance calculations. In contrast to the H3s and L3s, the LL3s are isotopically heavier than LL6s. This is not easily explainable with the metamorphic model, which should preferentially volatilize the lighter isotopes from hotter regions (types 4-6) to colder regions (type 3s) (Luck et al. 2005).

Rubidium seems to be fairly constant with petrographic type for H- and L-chondrites. There is only 1 abundance determination for an H3, so this variation is not considered significant. However, in the LL-chondrites, Rb is nearly twice as abundant in the type 3s as in the higher petrographic types. However, the uncertainties of all the petrographic types overlap, so it is uncertain if this is a real enrichment.

Tellurium is chalcophile and siderophile so Te should be present in both sulfide and metal (Allen and Mason, 1973). A comparison of S/Te ratios in H- (55,862), L- (58,112), and LL- (47,472) chondrites shows greater variability than the S/Se ratios of 2371 (H), 2375 (L), and 2433 (LL) and is consistent with some Te being in the metal phase. The median Te abundances in Tables 1-3 were used in these calculations, but a similar pattern emerges using the mean Te values. Goles and Anders (1962) report that Te is very susceptible to leaching, indicating that at least some of it is located in water-soluble phases, perhaps CaS, $FeCl_2$, and MgS. From Fig. 1, we can see that Te abundances are nearly constant with petrographic type in H- and L-chondrites. For H3 chondrites, there is only one very large Te abundance for Sharps H3.4 (3200 ng/g), and abundances in the H/L3s are essentially the same as those of the higher petrographic types, making an enrichment in the type 3s uncertain at best. However, Te abundances in LL-chondrites have a similar pattern to Se, although with more exaggerated variation, with LL3 and LL4 chondrites containing almost twice as much Te as LL5 and LL6 chondrites. The isotopic composition of Te in one L3 chondrite (Mezö-Madaras, $\delta^{126/128}$Te = 1.9±0.6‰) is of a similar order to the observed Zn isotopic compositions, although measurements for an H5 and an LL6 fall were isotopically normal (Fehr et al. 2005). While this may suggest isotopic fractionation due to metamorphism, a single measurement is inconclusive and more measurements of the Te isotopic composition in ordinary chondrites should be made.

Silver is slightly more variable than Rb and Te. In the higher petrographic types, the abundance of Ag is relatively constant in each of the ordinary chondrite classes, which agrees with the results of Wolf and Lipschutz (1998). However, Ag seems to be consistently enriched in all of the type 3 ordinary chondrites. Unfortunately, the low number of Ag analyses for type 3 chondrites (1 H, 2 L, 4 LL) and overlap in uncertainties with the higher petrographic types means

that we cannot determine if this is a real difference. However, as with Zn and Cu, the isotopic composition of Ag is variable ($^{107}Ag/^{109}Ag$ varies by about ~1‰) (Schönbächler et al. 2008). This variability is only partially due to radioactive decay of ^{107}Pd. The isotopic composition does not correlate with concentration, class or petrographic type. However, ordinary chondrites are consistently enriched in the heavier isotopes of Ag, which suggests that there was evaporative loss, possibly during open system thermal metamorphism (Schönbächler et al. 2008).

Figure 1 shows that the elements Cs and Bi are much more variable in abundance with petrographic type than the elements discussed above. Cesium shows a distinct decrease in abundance with petrographic type for both the H- and L-chondrites. This agrees with the results of Wolf and Lipschutz (1998), who concluded that the Cs abundance decreased with increasing petrographic type in equilibrated (4 – 6) H-chondrites. In the H-chondrites, the group of H3s and H/L3s is enriched in Cs by 1.2x, 2.8x, and 5.2x the Cs abundance of the H4s, H5s, and H6s, respectively. In the L-chondrites, L3s contain 2.5x, 15x, and 31x more Cs than the L4s, L5s, and L6-chondrites, respectively. The Cs abundance in the LL-chondrites does not follow such a neat trend. Only 5 analyses are available for type 5 LL-chondrites, and the low mean seems to be due to one analysis for Cherokee Springs with an especially low Cs abundance of 1.43 ng/g. If this analysis is eliminated, the error decreases significantly, and the geometric mean abundance becomes very similar to that for the type 4 and type 6 chondrites. Therefore, the type 3 LL-chondrites may contain about twice as much Cs as the higher petrographic types, but the error on the abundances overlap sufficiently to make the difference uncertain.

Bismuth is also enriched in type 3 chondrites relative to the higher petrographic types for each of the ordinary chondrite classes. In H-chondrites, petrographic types 4 – 6 have essentially constant abundances. For the H3 chondrites, we have only 2 analyses of the Bi abundance.

However, the abundance for H/L3 chondrites falls between the type 3 H-chondrites and the higher petrographic types, which indicates that the abundance in the H3 is not unreasonable since H/L chondrites should have lower siderophile abundances than corresponding H chondrites. Taken together, the H3s and H/L3s have ~13x more Bi than the H4-H6 chondrites. Figure 2a shows that the H3s and H/L3s have a decreasing Bi abundance with increasing petrographic type from 3.4 to 3.9. No such trend is observed for the L- or LL-chondrites. In L-chondrites, Bi abundances in type 3s are ~5x and ~18x larger than in types 4 and 5. Type L6 chondrites have approximately the same abundance as L5s. In LL-chondrites, although there is some scatter and significant error, it seems that the higher petrographic types (4-6) have essentially constant abundance, with type 3 chondrites having ~4x more Bi.

There are few bulk abundance determinations for Ge, Pb, and Sn in ordinary chondrites. For Ge, there seems to be a nice trend of decreasing abundance with petrographic type from type 4 to 6 in H-chondrites, whereas the abundance in L-chondrites is essentially constant. For LL-chondrites, there are only 5 abundance determinations, which scatter widely. The Pb in chondrites is subject to significant contamination from terrestrial sources, so the indigenous abundance of Pb is difficult to determine (Unruh, 1982). The abundance of lead is best determined in H-chondrites with 13 analyses for types 4 – 6. The Pb abundance seems to be relatively constant with petrographic type. Although we would expect Pb to behave similar to Bi and be enriched in the type 3 chondrites, there are no bulk abundance determinations that can be used to prove this. Tin analyses are also subject to analytical problems (Buseck, 1971). For Sn there are analyses only for 2 H/L3, 2 H5, 1 L3, 3 L6, and 1 LL3 chondrites, which are not enough to determine petrographic trends.

3.1.2. Highly Volatile Elements (Cd, Br, In, I, and Tl). All of the highly volatile elements seem to be enriched in the lower petrographic types, as can be seen in Fig. 1. For Cd, the H4-H6 chondrites have essentially constant abundances. There are no analyses for Cd in the H3-chondrites, but the H/L3 chondrites contain ~9x more Cd than the H4-H6 chondrites. The H/L3 chondrites typically have lower concentrations of siderophiles than the H3 chondrites (e.g., see As, Au, Cu, Ag, Rb, Cs, Bi, Se, In, Tl), so we would expect the H3 chondrites to have significantly larger Cd abundances than the H4-H6 chondrites. In L-chondrites, both the L3 and L4 types are enriched over the L5 and L6 chondrites. Averaged together, the L3+L4 group contains 4x more Cd than the L5+L6 group. In LL-chondrites, the mean Cd abundances decrease significantly with increasing petrographic type, and the LL3s contain 2x, 5.5x, and 8.5x more Cd than the LL4s, LL5s and LL6s, respectively. Cadmium also has a highly variable stable isotope composition (Wombacher et al. 2003, 2008). Unequilibrated ordinary chondrites have much wider variations in the Cd isotopic composition (~23‰) compared to equilibrated ordinary chondrites (~3.5‰). These variations are much larger than those for Cu, Zn, or Ag discussed above, as expected based upon the higher volatility of Cd. Like Ag, Cd in ordinary chondrites is enriched in the heavier isotopes, which suggests evaporative loss. Wombacher et al. (2008) suggest that the wide variation in Cd isotopes is a result of multiple episodes of partial condensation and volatilization associated with thermal metamorphism.

Bromine decreases with increasing petrographic type in H-chondrites. The abundance of Br in the H3 chondrites and the H/L3 chondrites is nearly identical, and is 4x, 10x, and 13x greater than the H4s, H5s, and H6 chondrites, respectively. However, there are few analyses of Br in ordinary chondrites, so the differences between the petrographic types are hard to quantify. In L-chondrites, the abundance of Br decreases from type 3 to type 5. The abundance of Br in L5

and L6 chondrites is similar. The enrichment of Br in the L3s is 2.5x L4s and 5.5x (L5s+L6s). In LL-chondrites the abundance of Br is roughly 3.5x greater in the type 3 and 4 petrographic types than in types 5 and 6. There are only 2 abundance analyses for Br in LL4 chondrites, so this abundance is very uncertain.

Indium abundances for H4 - H6 chondrites are approximately constant but those in H3 and H/L3 chondrites are significantly higher and decrease with increasing petrographic type, as shown in Fig. 2a. The average enrichment of the H3s + H/L3s is nearly 38x the In abundance in H4-H6. Similarly, in LL-chondrites, the In abundance in type 3 chondrites is nearly 12x greater than in the LL4-LL6-chondrites. Figure 2b shows that In decreases with increasing petrographic type from 3.0 to 3.6 in the LL-chondrites, with the exception of two large values for Chainpur (LL3.4). The reason for this discrepancy is unknown. In L-chondrites, the mean In abundances decrease from L3 to L5 chondrites and the L5 and L6 chondrites have essentially constant In abundances. The In abundance in L3 chondrites is 4x greater than in L4s and ~64x greater than in L5s and L6s. Abundances of In within the L3 chondrites do not show any trends with petrographic type. Thallium abundances (like those of Bi, Cd, Br, and In) are ~3x larger in H3s than in H4 – H6 chondrites. Figure 2a shows that, like Bi and In, Tl decreases with increasing petrographic type for the H3s and H/L3s. The LL3 chondrites have ~13x more Tl than higher petrographic types, and decrease with increasing petrographic type (Fig. 2b). In L-chondrites, Tl shows broadly similar behavior to Cd. Thallium abundances are ~3x larger in the L3s and L4s than in the L5s and L6s.

There are very few analyses of bulk iodine in ordinary chondrites. Only 1 analysis is available for H-chondrites, 3 for L-chondrites and none for LL-chondrites. There is no way to

establish if there are any abundance trends for iodine. More analyses of this element need to be done.

3.2 Interpretations of Trace Element Patterns

We can see from looking at Figure 1 that the abundances of the moderately volatile elements in ordinary chondrites are not simply controlled by their volatility in the solar nebula. Depletions of the trace elements relative to CI chondrites should become greater from left to right across Fig. 1 if the elemental abundances are controlled by volatility in the solar nebula. However, there is no simple trend of decreasing abundance with decreasing condensation temperature. Additionally, trends with petrographic type do not correlate simply with solar nebula volatility either. The moderately volatile elements As, Au, Cu, Sb, Ga, Zn, and Se have essentially constant abundances with petrographic type in all of the ordinary chondrites, as expected from their solar nebula volatility, and the highly volatile elements Cd, Br, In, and Tl are enriched in the lower petrographic types, also as expected from their solar nebula volatility. However, the moderately volatile elements Ag, Rb, and Te have minor abundance variations, and Cs and Bi are highly enriched in lower petrographic types. If solar nebula volatility controlled the abundance patterns of these elements, we would not expect to see such enrichments. One possible interpretation of these abundances is that the distribution of these elements has been altered by parent body processes controlled by their volatility and mobility within that environment.

For several of the highly variable elements (Bi, In, Tl), trends were observed within the H3 and H/L3 petrographic types (see Fig. 2a), and the LL3 chondrites (In, Tl) (Fig. 2b). If we look at Fig. 1, these are the elements for which the type 3s are greatly enriched over the higher petrographic types, which have nearly constant composition rather than a gradual decrease in

abundance. We found no such trends for the L-chondrites, which from Fig. 1 is not surprising. The only element which shows this pattern in L-chondrites is Ag, for which we have only 2 analyses for type L3 chondrites. We might also have expected to see similar trends for Cd in H-chondrites and Bi in LL-chondrites. However, there are no analyses for Cd in H3 chondrites, and only 3 in H/L3 chondrites. For Bi in LL3 chondrites, no regular pattern is found with increasing petrographic type.

Interpreting the observed abundance patterns within the terms of the metamorphic volatilization model suggests that the elements were mobilized to different degrees in the different ordinary chondrite parent bodies. In the H-chondrite parent body, Bi, Cd, In, and Tl seem to have been completely mobilized from the interior (types 4-6) to the outer, cooler edges of the parent body (types 3), whereas Cs, Br, and possibly Ag were mobilized to a lesser degree. In the L-chondrite parent body, enrichments in Cs, Bi, Cd, Br, In, and Tl, and possibly Ag, indicate that they were mobilized to the outer layers of the parent body (types 3 and 4) but not to the same extent as in the H-chondrite parent body. In the LL-chondrite parent body, In and Tl seem almost completely mobilized to the exterior, while Br, Cd, Bi, Cs, and possibly Ag, Rb, and Te, were mobilized to a lesser extent. If we assume that chemistry within the parent bodies was similar, this may suggest a volatility sequence: that In and Tl were the most volatile, followed in order of decreasing volatility by Bi and Cd, Cs and Br, Ag, Rb, and Te, and followed by As, Au, Cu, Sb, Ga, Zn, and Se in no particular order. Unfortunately, we are not able to say anything about the volatilities of Pb, Ge, Sn, or I based on their abundance patterns. We will compare this volatility sequence to our results given below.

4. Methods

We used chemical equilibrium calculations to model volatile element chemistry during metamorphism of ordinary chondritic material. We did chemical equilibrium calculations using a Gibbs energy minimization code of the type described by Van Zeggern and Storey (1970). Our calculations consider major rock-forming elements (Al, Ca, Fe, K, Mg, Na, O, Si, Ti), minor elements (Co, Cr, Mn, Ni, P, S), trace elements (Cu, Zn, Ga, Ge, As, Se, Rb, Ag, Cd, In, Sn, Sb, Te, Cs, Au, Tl, Pb, Bi), and volatiles (C, Cl, F, H, N, Br, I) in chondrites. We used the IVTANTHERMO database (Belov et al., 1999), to which we added a number of minerals found in chondrites. Approximately 1700 compounds of 40 elements were included in the calculations. Our nominal model uses ideal solid solutions of olivine $(Mg,Fe,Zn,Mn)_2SiO_4$, pyroxene $(Mg,Ca,Fe,Zn,Mn)SiO_3$, feldspar $(Na,K,Ca)_2(Al,Si)_3SiO_8$, and metal (Fe, Ni, Co). For the trace elements, we did calculations in which we considered both (1) that solid phases were pure compounds of the elements and (2) that the trace elements formed solid solutions with the major elements. In reality, most trace elements in meteorites typically do not form discrete minerals, but dissolve in more abundant host phases or are dispersed among several phases. However, the thermodynamic properties of trace element solid solutions in the host minerals are generally unknown; therefore, we used ideal solid solutions (i.e., activity coefficients $\gamma_i = 1$). Where estimates of the activity coefficients can be made, we discuss their effects on our calculations.

A note about terminology: although our calculations are methodically the same as equilibrium condensation calculations (see e.g. Lodders 2003), we use the term "formation temperature" (T_f) in describing our results in order to distinguish between the different environments of the solar nebula, where condensation takes place, and the meteorite parent bodies, where the elements are mobilized by metamorphism. Because we are doing chemical equilibrium calculations, the initial siting of the elements does not affect the final result; in fact,

we make no assumptions about the phases that elements initially occupy. (In other words, the results of chemical equilibrium calculations are path-independent because changes in Gibbs energy, which is a state function, are path-independent. We refer the reader to Lewis and Randall (1961) or another text in chemical thermodynamics for further clarification of the concepts of state functions and path-independence.) All mineralogy is a direct result of the equilibrium calculations.

We used temperature (300 – 3000 K) and pressure (10^{-4} – 100 bar) ranges appropriate for P – T profiles within possible meteorite parent bodies (i.e., asteroids). Generally, within a closed metamorphic system, the total pressure at depth is equal to the lithostatic pressure (Spear, 1995), which approaches the kilobar range for large bodies. The lower pressures used in our calculations are more suitable for surface conditions, or an open system with very large porosity. We discuss calculation of P - T profiles for the asteroid *6 Hebe*, a prime candidate for the H – chondrite parent body, in our earlier paper (Schaefer and Fegley, 2007a). Lodders (2003) describes details of thermodynamic calculations for gas – solid chemical equilibria.

We used the average major element compositions of H-, L-, and LL-chondrites in Table 1 of Schaefer and Fegley (2007a) for our nominal models. We used the median trace element abundances given in Tables 1-3 of the present paper as the nominal abundances in our model. As discussed by Lodders (2003), the 50% T_c of a trace element is independent of its total abundance because its chemistry is dictated by the major elements, so we do not consider the effect of trace element abundance on the 50% T_f (where 50% of an element is in the gas and 50% in condensed phases).

5. Results

Table 4 summarizes our results for H-chondritic material. It lists the 50% T_f of solid phases for each of the trace elements considered in our calculations at total pressures of 1 bar and 10^{-4} bar for both the pure phase calculations and the ideal solid solution calculations. Pure phase calculations can be taken as lower limits, and the solid solutions as upper limits. It should be noted that the solid solution calculations give results for most of the elements above the metamorphic temperatures of ordinary chondrites (<1300 K), and also above the liquidus temperatures of chondritic material [e.g., T_{liq}(CAIs) ~1800 K, Stolper (1982)]. We do not consider molten solutions because the ordinary chondrites were never melted. However, our calculations define a range of possible volatilities for each element.

In Table 4, we also compare our calculations to the 50% T_c of the trace elements in the solar nebula, which are significantly different. Formation temperatures of the major elements are also significantly different. For instance, in Fig. 3 and 4, we show the 50% T_f of Fe (metal) and FeS (troilite), which are 1812 K and 1524 K, respectively, at 10^{-4} bar. These temperatures are significantly higher than their 50% T_c in the solar nebula of 1334 K and 664 K, respectively (Lodders, 2003). The differences in condensation temperature are entirely due to compositional differences. The solar nebula is overwhelmingly dominated by hydrogen, and other elements are kept in the gas phase to much lower temperatures due to reactions with hydrogen. For example, sulfur chemistry in the solar nebula is dominated by H_2S (g). In contrast, the H-chondrite is hydrogen-poor in comparison to the solar nebula and H_2S (g) is much less abundant, which allows FeS (troilite) to form at higher temperatures. Since the trace element chemistry is governed by that of the major elements, we expect the volatility sequence of the trace elements to be significantly different in H-chondritic material than in the solar nebula. For a full discussion of the major element chemistry, see our previous paper (Schaefer and Fegley 2007a).

Figures 3 – 5 show the 50% T_f of the trace elements in H-chondritic material as a function of total pressure. We show results for both (a) the pure phase calculations and (b) ideal solid solutions. The temperature and pressure profile for the nominal H-chondrite parent body *6 Hebe* (Schaefer and Fegley, 2007a) is shown for comparison. The shaded regions show a range of melting temperatures for ordinary chondritic material. At higher temperatures, the material is liquid, and the ideal solid solution model is no longer applicable. We discuss results for each element below based upon the phases into which they dissolve in the meteorite (metal, sulfide, and plagioclase).

Results for the pure phase calculations are not significantly different for the L- or LL-chondritic material. Formation temperatures in the solid solutions differ due to the different abundances of Fe metal and total Fe in the different ordinary chondrites. In the L-chondrites, metal contains at most 35% of the total iron, with an initial T_f of 2830 K at 1 bar, and FeS has a 50% T_f (for S) of 2556 K. In the LL-chondrites, Fe metal contains at most 17% of total Fe, with an initial T_f of 2740 K, and FeS has a 50% T_f of 2540 K, similar to that of L-chondrites. For the trace elements dissolved in the metal, 50% T_f in H-chondrites are higher by ~100-200 K than in L-chondrites, and are ~200-400 K greater than in LL-chondrites. For the sulfides, the 50% T_f are similar in all ordinary chondrites, varying by <100 K as a whole, with the exception of InS and Tl_2S, which have 50% T_f that are ~300 K (InS) and ~100 K (Tl_2S) lower in the LL-chondrites than in the H- and L-chondrites. The 50% T_f for the majority of the sulfides varies by <30 K, with the L-chondrites generally having the highest 50% T_f. The 50% T_f of the silicates (Rb and Cs) differ by less than 40 K amongst the ordinary chondrites. For the sake of brevity, we do not discuss the results for L- and LL-chondrites in detail below.

5.1 Formation Temperatures of Solid Phases of the Trace Elements in H-chondrites

5.1.1 Metal Figure 3 shows the 50% T_f of Fe metal and the trace elements As, Ag, Au, Bi, Cu, Ga, Ge, In, Pb, Sb, Sn, and Tl as a function of pressure. Figure 3a shows these elements as pure phases, and Fig. 3b shows their 50% T_f when they are dissolved in Fe metal (or FeS for the sulfide compounds). The formation temperature curve for Fe metal is the same in both Fig. 3a and 3b because Fe is not affected by the chemistry of the trace elements. However, as can easily be seen, dissolving the trace elements in metal significantly increases their formation temperatures over pure phases. In general, the solid solutions are typically more pressure dependent than the pure phases. We discuss each element below.

In the pure phase calculations, Ag, As, Au, Bi, Ge, and Sb form metals. However, their formation temperatures increase drastically when they are allowed to form ideal solid solutions with Fe metal: +1543 K (Ag), +1620 K (As), +1372 K (Au), +1644 K (Bi), +913 K (Ge), +1887 K (Sb). Estimates of activity coefficients can be made for these elements. For As, Au, Ge, and Sb, we use activity coefficients from Wai and Wasson (1979). The non-ideal activity coefficients raise the 50% T_f of As, Ge, and Sb by 90 K, 425 K, and 38 K, so the 50% T_f in Fig 3b for these elements should be taken as a lower limit for solid solutions. However, the difference between pure phases and ideal solid solutions is much more significant than the affect of the activity coefficient on the 50% T_f.

On the other hand, Au, Ag and Bi are highly incompatible with Fe metal, so they have very large activity coefficients, which should lower their 50% T_f considerably (Wai and Wasson 1977, Chang and Schlesinger, 1998; Wriedt et al. 1973). The activity coefficient for Au from Wai and Wasson (1977) is γ_{Au}= 5, and lowers the 50% T_f of Au by 60 K at 1 bar. The activity coefficient for Bi in γ-Fe is on the order of 10^4 at temperatures of 1473 – 1673 K, with a temperature dependency given by the equation

$$\ln \gamma_{Bi} = \frac{1.53 \times 10^4}{T} + 0.314 \pm 0.25 \quad (1)$$

(Chang and Schlesinger, 1998). If we use an estimated value for γ_{Bi} of 10^4, the 50% T_f of Bi metal drops to 1245 K at 1 bar. However, if we extrapolate the temperature dependence of the activity coefficient to much lower temperatures, which may arguably not be a valid extrapolation, Bi does not condense as metal at any temperature. Silver has a smaller activity coefficient than Bi in γ-Fe, given by the equation

$$\ln \gamma_{Ag} = \frac{1.38 \times 10^4}{T} - 5.27 \quad (2)$$

from 1366 to 1561 K (Wriedt et al. 1973). At 1 bar pressure, if we use an average value for γ_{Ag} of 50, which is the value at 1500 K, then the 50% T_f drops to 2185 K. Therefore, the curves for Au, Ag and Bi in Fig. 3b should be considered upper limits. Silver and Bi may prefer to enter the sulfide rather than the metal. Shown in Fig. 4b are 50% T_f curves for Ag_2S and Bi_2S_3 dissolved in the sulfide phase, which have 50% T_f at 1 bar of 2366 K and 981 K, respectively. This is a substantial reduction in volatility for Bi.

In the pure phase calculations, Sn (s) forms at 828 K at 1 bar. At lower temperatures, Sn (s) converts into herzenbergite SnS at a temperature of ~600 K, independent of pressure, via the net thermochemical reaction

$$\text{Sn (metal)} + H_2S\ (g) = \text{SnS (herzenbergite)} + H_2\ (g) \quad (3)$$

At the pressures lower than ~10^{-3} bar, Sn (metal) is not a stable phase, and SnS is the first Sn-bearing phase to form. However, this is an unlikely scenario, as most Sn in ordinary chondrites is found in the metal phase in ordinary chondrites (Fehr et al. 2005). When Sn dissolves in Fe metal, its 50% T_f is 2300 K, an increase of 1472 K at 1 bar, assuming ideal solid solution. However, the Sn-Fe binary alloy system shows positive deviations from ideality, which increase

with decreasing Sn content and decreasing temperature (e.g. Eric and Ergeneci 1992; Fedorenko and Brovkin 1977). If we estimate $\gamma_{Sn} = 2$, the 50% T_f of Sn in Fe metal drops to 2209 K. This temperature should be considered an upper limit.

In contrast to the elements discussed above, Cu, Ga, In, Pb, and Tl do not initially form as metals in the pure phase. Copper forms as chalcocite Cu_2S (s) at 1952 K at 1 bar total pressure. Chalcocite Cu_2S (s) converts into copper metal at 895 K, independent of pressure, via the net thermochemical reaction

$$Cu_2S \text{ (chalcocite)} + H_2 = 2Cu \text{ (metal)} + H_2S \quad (4)$$

In the solid solution, Cu dissolves in metal at 2839 K, assuming ideal solid solution. This is an increase of 887 K over the pure phase 50% T_f. Using a non-ideal activity coefficient for Cu from Wai and Wasson (1979), the 50% T_f drops by 64 K, to 2775 K, which is not a significant change. In the pure phase, gallium condenses into Ga_2O_3 (s) at 1111 K at 1 bar. In the ideal solid solution, Ga dissolves into metal at 2670 K, which is an increase of 1559 K. Using a non-ideal activity coefficient from Wai and Wasson (1979), the 50% T_f increases by 48 K. In many natural systems, Ga can substitute for Al in silicates such as plagioclase. However, using ideal solid solution, we did not find Ga to be stable in plagioclase for the H-chondrite system.

Indium, lead and thallium condense as InS (s), PbSe (s) and TlI (s) in the pure phase calculations. Their 50% T_f at 1 bar in H-chondritic material are 492 K, 772 K, and 475 K, respectively. In the ideal solid solution calculations, all three elements initially go into the metal at 1 bar pressure at temperatures of 2605 K, 2355 K, and 2225 K, respectively. The 50% T_f increase by 2113 K, 1583 K, and 1750 K, respectively. However, In, Pb, and Tl all have very low solubilities in Fe, and so the ideal solid solution calculation should be considered an upper limit (Okamoto 1990, Raghavan 2008, Wodniecki et al. 1999). Rather, In, Pb, and Tl may go

into the sulfide solid solution. The 50% T_f at 1 bar for InS, PbS, and Tl_2S are 1641 K, 1651 K, and 1781 K, respectively. These curves are shown in Fig. 3b.

5.1.2 Sulfide Figure 4 shows the 50% T_f of S and the trace elements Cd, Se, Te, and Zn as (a) pure phases and (b) solid solutions in FeS. Figure 5 shows the 50% T_f of Br and I, which also dissolve in FeS. In the pure phase calculation, Cd initially condenses as CdTe at 718 K at 1 bar. As the temperature decreases, CdTe converts into CdSe via a net thermochemical reaction such as

$$CdSe\ (s) + H_2Te\ (g) = CdTe\ (s) + H_2Se\ (g) \quad (5)$$

The 50% T_f of CdSe (465 K) is pressure independent. In the ideal solid solution calculation, Cd dissolves into both the metal and the sulfide phases. The 50% T_f curve of the metal phase is more pressure dependent than the sulfide. Therefore, at higher pressures (> 1 bar), Cd initially dissolves into the metal. At lower pressures, Cd dissolves first into the sulfide. At 1 bar the 50% T_f of Cd in the sulfide is 1406 K, which is an increase of 688 K above the pure phase calculation.

Zinc forms several compounds in the pure phase calculations. At pressures above ~10^{-2} bar, the initial zinc phase is ZnS, which is sphalerite at lower pressures and wurtzite at higher pressures. At 1 bar, the 50% T_f of ZnS is 1155 K. ZnS is converted into $ZnCr_2O_4$ at 945 K independent of pressure. At low pressures (<10^{-2} bar), $ZnCr_2O_4$ is the initial stable zinc phase. In the ideal solid solution calculations, we found that zinc dissolved primarily into the sulfide with a 50% T_f of 1716 K. At lower temperatures, Zn dissolved into silicates (olivine as Zn_2SiO_4 and enstatite as $ZnSiO_3$). If we take an estimated activity coefficient for ZnS in FeS of 10^3 from Wai and Wasson (1977), then the 50% T_f drops significantly to 840 K at 1 bar, which would make the silicates the more stable phase.

The initial stable phase for Se in the pure phase calculations is ZnSe, which contains < 15% of total Zn. Therefore, the 50% T_f curve for ZnSe in Fig. 4a shows the 50% T_f of Se, which is 875 K at 1 bar. PbSe, which is shown in Fig. 3a, and CdSe (Fig. 4a) both contain < 1% of all Se. Iron selenide forms at ~370 K via the net reaction

$$ZnSe\ (s) + FeCr_2O_4\ (chromite) = FeSe\ (s) + ZnCr_2O_4\ (s) \quad (6)$$

The formation of iron selenide destroys ZnSe. In the ideal solid solution calculations, Se dissolves in FeS as $FeSe_{0.961}$ at a temperature of 2302 K at 1 bar. The initial Te phase is $FeTe_{0.9}$ (s) at all pressures in the pure phase calculation. Its 50% T_f at 1 bar is 757 K. CdTe forms at a slightly lower temperature, but contains only ~1.5% of total Te. In the ideal solid solution calculations, Te dissolves in FeS as $FeTe_{0.9}$. At 1 bar, its 50% T_f is 1962 K, which is an increase of 1205 K.

Bromine and iodine, shown in Fig. 5, also dissolve in the sulfide in our solid solution calculations. In the pure phase calculations, Br is found in RbBr (s) at all pressures. Its 50% T_f at 1 bar is 843 K. RbBr contains only ~17% of total Rb, so the curve shown in Fig. 5a is for 50% condensation of Br. In the ideal solid solution, Br dissolves in the sulfide as $FeBr_2$. At 1 bar, $FeBr_2$ has a 50% T_f of 1397 K, an increase of 554 K. In the pure phase, I is found primarily in CsI, although small amounts of I are found in RbI and TlI. The 50% T_f of CsI is 742 K. Cesium and iodine have very similar abundances, so their 50% T_f lines are the same. In the ideal solid solution, I dissolves in the sulfide as FeI_2. FeI_2 has a 50% T_f of 1351 K. The 50% T_f of both $FeBr_2$ and FeI_2 are much more pressure dependent than the pure phases.

5.1.3 Plagioclase Figure 5 shows the 50% T_f of Rb and Cs as (a) pure phases and (b) solid solutions with plagioclase. Rb and Cs are found in water-soluble phases and feldspars in ordinary chondrites (Gast, 1960, 1962; Smales et al., 1964; Curtis and Schmitt, 1979; Wieler et al., 2000).

Thermodynamic data for Cs and Rb feldspars are unavailable so we could not include them in our pure phase calculations. However, a number of inorganic compounds of Rb and Cs are in the calculations (borates, carbonates, halides, hydrides, hydroxides, nitrates, nitrites, oxides, sulfides, sulfates). In our pure phase calculation, we found that Rb and Cs condensed as the halide salts RbCl (s,l), with minor amounts of RbBr (s,l) and RbI (s), and CsI (s), respectively. At a pressure of 1 bar, the 50% T_f for RbCl is 911 K, and for CsI is 742 K. Observations of Rb in sylvite in the Monahans (1998) H5 chondrite suggest that some Rb may partition into feldspar, possibly via exchange reactions such as

$$RbCl\ (\text{in sylvite}) + KAlSi_3O_8\ (\text{in feldspar}) = KCl\ (\text{in sylvite}) + RbAlSi_3O_8\ (\text{in feldspar}) \quad (7)$$

Similar reactions can be envisioned for Cs, but the work of Curtis and Schmitt (1979) shows that Cs can be dispersed among several phases in ordinary chondrites. In our ideal solid solution model, we approximated data for Rb and Cs feldspar using available data for $KAlSi_3O_8$. At 1 bar, Rb and Cs had 50% T_f in plagioclase of 971 K and 836 K, respectively. Compared to all of the other elements considered here, these are much smaller increases in formation temperatures. Due to the lack of thermodynamic data for these phases, this result is not considered robust.

6. Discussion

6.1 Volatility sequences

Table 5 lists the volatility sequences for the trace elements in order of increasing volatility for H -chondritic material at pressures of 1 bar and 10^{-4} bar for both pure phases and ideal solid solutions. The volatility sequences are derived from our results described above. Increasing volatility corresponds to decreasing formation temperatures for solid phases containing an element. The pure phase calculations and solid solution calculations define a range of possible volatilities for each element. Elements should not be less volatile than calculated with solid

solutions, or more volatile than in the pure phase calculations. To our knowledge, there are no other volatility sequences available for ordinary chondritic material. Fegley (1990) modeled volatile trace element transport during ordinary chondrite metamorphism, but only presented results for lead. Previous papers about the volatility of trace elements in ordinary chondritic material relied on the volatilities of these elements in the solar nebula (e.g. Larimer, 1967; Larimer and Anders, 1967). The solar nebula volatility (condensation) sequence calculated by Lodders (2003) is also listed in Table 5 for comparison. Lipschutz and colleagues measured the mobility of trace elements in heated chondritic material, and we discuss their work later.

As can be seen from Table 5, our calculated volatility sequences for trace elements in H-, -chondritic material are very different from that of the solar nebula. For the pure phase calculations, the volatilities of As, Sb, and, to a lesser degree, Bi and Cs in ordinary chondritic material are much higher than in the solar nebula. For the solid solution calculations, while the volatility of As is similar to the solar nebula, In and Bi are much less volatile than in the solar nebula, and Rb and Cs become the most volatile of all the elements considered. The elements which have highly non-ideal activity coefficients complicate the volatility sequences. The effect of non-ideality is largest for Ag, Ge, Bi, In, and Tl. Assuming non-ideality, Ge is less volatile than shown in Fig. 3b, whereas the other elements are significantly more volatile. Additionally, the 50% T_f of Rb and Cs are highly uncertain due to the lack of data for their solid solutions. Comparisons between the volatility sequence of the H-chondrites to the solar nebula should also take into account the differences in absolute volatility, which can be seen in Table 4. For the solid solution calculations, the 50% T_f of the ordinary chondrite are so much greater than those of the solar nebula that all of the elements, excepting Rb and Cs, would be considered refractory.

As we have previously discussed, differences in volatility between the solar nebula and ordinary chondrite parent bodies are not too surprising, considering the different compositions involved. The solar nebula composition is significantly more reducing, i.e., has a lower oxygen fugacity, at a given temperature than ordinary chondritic material ($\log f_{O_2}$ (solar neb.) ~ –27 vs. $\log f_{O_2}$ (H-chond.)~ –22 at 10^{-4} bar and 1000 K). The ordinary chondritic compositions are much more oxidizing, which alters the major gases and stable solid phases of the trace elements, and therefore the formation temperatures for the solid phases. As stated by Keays et al. (1971): "It is virtually certain that the condensation curves of [trace elements in the solar nebula] cannot be applied to metamorphic fractionations."

Table 5 also lists a volatile mobility sequence for the unequilibrated ordinary chondrite Tieschitz (H/L3.6) as measured by Ikramuddin et al. (1977). Ikramuddin et al. (1977) heated samples of Tieschitz in a stepped fashion in an atmosphere of 10^{-5} atm H_2 for temperatures of 400˚ – 1000˚C and measured the amounts of volatile elements retained after heating. Nearly all Cs, Bi, Tl, Ag, In, Te, and Zn are lost from the samples at the end of the heating run, whereas most Ga and Se remain. The mobility of thermally labile elements is governed more by kinetic factors such as diffusion and desorption than by thermodynamics (Ikramuddin et al. 1977), making comparisons to our calculated volatility sequences problematic. However, the comparison is an instructive one, showing that elements that we calculate to be stable within an ordinary chondrite parent body, such as Ag and Zn, may, in fact, move around during open system metamorphism.

We did calculations for conditions comparable to the experimental conditions of Ikramuddin et al. (1977) (P~10^{-5} bar, T=300-1300 K), in order to determine if the differences between the calculated volatilities and the observed mobility sequence are due to differences in

pressure. For pure phases, we found that Ag and Zn became significantly more volatile, whereas the volatility of the other elements considered by Ikramuddin et al. (1977) did not change considerably. The initial formation temperature for Ag metal dropped from 1176 K at 1 bar to 840 K at 10^{-5} bar, and the 50% formation temperature of Zn (as $ZnSiO_3$ in enstatite solid solution) dropped from ~1500 K at 1 bar to ~850 K at 10^{-5} bar. For the solid solution calculations, if we extend Fig. 3b-5b out to 10^{-5} bar, we can see that all of the elements in the experiment are at least somewhat volatile within this temperature region with the exception of Ag, Ga, and Se. The results of the experiment suggest that Ga and Se should not be volatile; however, Ag remains much more refractory than the experiment shows. Even using our estimated value for the activity coefficient of Ag, the metal is only very slightly volatile within the range of metamorphic temperatures, and the sulfide Ag_2S not at all.

6.2 Comparison to Trace Element Patterns and Implications for Parent Body Metamorphism

During closed-system metamorphism, a meteorite parent body retains its initial complement of volatile elements and redistributes it. Volatile trace elements are mobilized from layers at high temperature to colder layers, which enriches the lower petrographic types in volatile elements relative to the higher petrographic types. During open-system metamorphism, volatile elements can be lost from the system. Abundances of the volatile elements in the higher petrographic types are depleted relative to their initial abundances, whereas the abundances in the lower petrographic types may represent a combination of both redistribution and volatile loss. Volatile loss will be governed by the vapor pressure of the element, since any vapor can be lost from the system. Our calculated volatilities can represent a proxy for the vapor pressure (the 50% T_f represents the temperature at which 50% of the element remains in the gas, and 50% is in a condensed phase). The element can be lost at temperatures above the 50% T_f, and slightly below,

until it completely enters the condensed phase. In our calculations, closed system metamorphism can be approximated by the equilibrium calculations at high pressures, which correspond to lithostatic pressures within asteroid-sized parent bodies with low porosities. Open systems will have much larger porosities, and will therefore correspond to calculations at lower pressures (< 1 bar).

From our pure phase model, we predict that the elements Rb, Cu, Au, Ag, Zn, and Ga should be unaffected by closed-system thermal metamorphism within an H-chondrite parent body similar to *6 Hebe* due to their low volatility and the high formation temperatures of their solid phases. The elements that are more volatile should be more easily vaporized and transmitted throughout the parent body during thermal metamorphism. These are the elements that should have highly variable abundances with petrographic type. According to our calculations, these elements include Tl, In, As, Sb, Bi, Cs, Te, Br, I and Cd, whereas Sn, Pb, Ge, and Se should be only moderately affected by closed-system metamorphism. However, the trace abundance patterns discussed in Section 3 suggest that Ag should be more volatile than we calculate, whereas As and Sb should be less volatile. In an open system at lower pressures, nearly all of the elements will be at least somewhat mobile, with Cu, Zn, Au, Ag, and Ga being the least affected. For open system metamorphism, we would therefore expect that all of the elements would have more variable abundances.

From our solid solution model, we found only Rb and Cs were volatile within the P and T conditions of the *6 Hebe* asteroid model. Thus, if the asteroid is a closed system, then we would expect no effect from thermal metamorphism on the abundances of the trace elements, with the exception of Rb and Cs. However, isotopic compositions of Cd, Zn, Cu, and Ag all support mobilization by metamorphism (Luck et al. 2005; Schönbächler et al. 2008; Wombacher et al.

2003,2008). In the case of open system metamorphism, other elements would be volatilized, including Br, I, Cd, Zn, Tl, In, Pb, Bi, and to a lesser degree, Te, Sn and Ge. However, even using our estimated value for the activity coefficient of Ag at 10^{-4} bar, the 50% T_f (1355 K) of Ag is still higher than the observed metamorphic temperatures, which makes it difficult to explain the variability in its abundance. Additionally, the relatively constant abundance of Zn is difficult to resolve with its calculated volatility and its variable isotopic composition, which is consistent with loss through metamorphic volatilization (Wombacher et al. 2005). Zinc and Te have similar depletions relative to CI chondrites, which is expected from their similar volatilities in the solar nebula. However, Te has more variable abundances, particularly in the LL-chondrites, although it is less volatile than Zn in solid solutions.

7. Conclusions

Trace element abundance patterns suggest that the elements were mobilized in the order In, Tl > Bi, Cd, Pb? > Cs, Br, Sn?, I?, Ge? > Ag, Rb, Te > As, Au, Cu, Sb, Ga, Zn, Se. (Lack of abundance data for Pb, Sn, I, and Ge makes it impossible to establish whether they are enriched in the lower petrographic types. We estimate their placement based upon similar geochemical behavior.) The elemental abundance trends suggest that mobilization was most extensive in the H-chondrite, and least in the L-chondrites. This may be consistent with thermal models for the ordinary chondrite parent bodies based on Pb-Pb ages which suggest that the L-chondrite parent-body was significantly larger than the parent bodies of the H- and LL-chondrites (Bouvier et al. 2007). The measured element mobilities are significantly different than their calculated volatilities at the possible pressure and temperature conditions within a closed parent body. Open system metamorphism, that is a system with much lower internal pressures due to large porosity, may more readily explain the variations in elemental abundances using our ideal solid solution

model. However, ideal solid solutions do not explain the variable abundances of all of the elements. In particular, Ag and Zn are difficult to explain. Both Ag and Zn have been shown to be mobile elements (Ikramuddin et al. 1977). However, the mobility of Ag is at odds with its calculated volatility from solid solutions, whereas the abundances of Zn in the different petrographic types are constant, which argues for total depletion of Zn in all petrographic types through vaporization. This is at odds with abundance trends for elements such as In, Tl, and Cd, which are more volatile than Zn, yet which show enrichments in the higher petrographic types rather than bulk depletions. Future models of parent body metamorphism need to explain these discrepancies.

8. Acknowledgements

We acknowledge support from the NASA Astrobiology and Outer Planets Research Programs and the McDonnell Center for the Space Sciences. We thank J. Friedrich, K. Lodders, and S. Wolf for helpful discussions, and H. Palme and J. Wasson for thorough reviews.

9. References

Allen, R. O., Jr., Mason, B. 1973. Minor and trace elements in some meteoritic minerals. Geochim. Cosmochim. Acta 37, 1435 – 1456.

Barshay, S. S. 1981. Combined Condensation-Accretion Models of the Terrestrial Planets. Ph.D. thesis, MIT, Cambridge.

Belov, G. V., Iorish, V. S., Yungman, V. S. 1999. IVTANTHERMO for Windows – database on thermodynamic properties and related software. CALPHAD 23, 173 – 180.

Binz, C. M., Ikramuddin, M., Rey, P., Lipschutz, M. E. 1976. Trace elements in primitive meteorites. VI. Abundance patterns of thirteen trace elements and interelement relationships in unequilibrated ordinary chondrites. Geochim. Cosmochim. Acta 40, 59-71.

Bouvier, A., Blichert-Toft, J., Moynier, F., Vervoort, J. D., Albarède, F. 2007. Pb-Pb dating constraints on the accretion and cooling history of chondrites. Geochim. Cosmochim. Acta 71, 1583-1604.

Buseck, P. 1971. Tin. *In*: Handbook of Elemental Abundances in Meteorites. (Mason, B., ed.) Gordon and Breach: New York, 377-386.

Chang, L., Schlesinger, M. E. 1998. Solubility of bismuth in γ-iron. Metall. Mat. Trans. 29B, 1371 – 1372.

Curtis, D. B., Schmitt, R. A. 1979. The petrogenesis of L-6 chondrites: insights from the chemistry of minerals. Geochim. Cosmochim. Acta 43, 1091 – 1103.

Dennison, J. E., Lipschutz, M. E. 1987. Chemical studies of H chondrites. II. Weathering effects in the Victoria Land, Antarctic population and comparison of two Antarctic populations with non-Antarctic falls. Geochim. Cosmochim. Acta 51, 741-754.

Dreibus, G., Wänke, H. 1980. On the origin of the excess of volatile trace elements in the dark portion of gas-rich chondrites. Meteoritics 15, 284 – 285.

Eric, R. H., Ergeneci, A. 1992. High temperature phase relations and thermodynamics in the iron-tin-sulphur system. Min. Eng. 5, 917-930.

Fedorenko, A. N., Brovkin, V. G. 1977. Vapor pressure of tin and thermodynamic properties of the tin-iron system. Sb. Nauchn. Tr. – Gos. Proektn. Nauchno-Issled. Inst. “Gipronikel” 3, 83-89.

Fegley, B., Jr. 1990. Chondrite metamorphism: Models of volatile trace element transport. Meteoritics 25, 364.

Fehr, M. A., Rehkamper, M., Halliday, A. N., Wiechert, U., Hattendorf, B., Gunther, D., Ono, S., Eigenbrode, J. L., Rumble, D. 2005. Tellurium isotopic composition of the early solar system – A search for effects resulting from stellar nucleosynthesis, 126Sn decay, and mass-independent fractionation. Geochim. Cosmochim. Acta 69, 5099-5112.

Friedrich, J. M., Wang, M.-S., Lipschutz, M. E. 2003. Chemical studies of L chondrites. V: Compositional patterns for 49 trace elements in 14 L4-6 and 7 LL4-6 falls. Geochim. Cosmochim. Acta 67, 2467-2479.

Friedrich, J. M., Bridges, J. C., Wang, M.-S., Lipschutz, M. E. 2004. Chemical studies of L chondrites. VI: Variations with petrographic type and shock-loading among equilibrated falls. Geochim. Cosmochim. Acta 68, 2889-2904.

Gast, P. W. 1960. Alkali metals in stone meteorites. Geochim. Cosmochim. Acta 19, 1-4.

Gast, P. W. 1962. The isotopic composition of strontium and the age of stone meteorites – I. Geochim. Cosmochim. Acta 26, 927-943.

Goles, G. G. 1971. Potassium. *In*: Handbook of Elemental Abundances in Meteorites. (Mason, B., ed.) Gordon and Breach: New York, 146-169.

Goles, G. G., Anders, E. 1962. Abundances of iodine, tellurium and uranium in meteorites. Geochim. Cosmochim. Acta 26, 723 – 737.

Hart, S. R., Zindler, A. 1986. In search of a bulk Earth composition. Chem. Geol. 57, 247-267.

Huston, T. J., Lipschutz, M. E. 1984. Chemical studies of L chondrites. III. Mobile trace elements and $^{40}Ar/^{39}Ar$ ages. Geochim. Cosmochim. Acta 48, 1319-1329.

Ikramuddin, M., Matza, S., Lipschutz, M.E. 1977. Thermal metamorphism of primitive meteorites. V. Ten trace elements in Tieschitz H3 chondrite heated at 400° - 1000° C. Geochim. Cosmochim. Acta 41, 1247 – 1256.

Kallemeyn, G. W., Rubin, A. E., Wang, D., Wasson, J. T. 1989. Ordinary chondrites: Bulk compositions, classification, lithophile-element fractionations, and composition-petrographic type relationships. Geochim. Cosmochim. Acta 53, 2747-2767.

Kargel, J. S., Lewis, J. S. 1993. The composition and early evolution of Earth. Icarus 105, 1-25.

Keays, R. R., Ganapathy, R., Anders, E. 1971. Chemical fractionations in meteorites. IV. Abundances of fourteen trace elements in L-chondrites; implications for cosmothermometry. Geochim. Cosmochim. Acta 35, 337-363.

Koblitz, J. 2005. METBASE Version 7.1 for Windows.

Larimer, J. W. 1967. Chemical fractionations in meteorites – I. Condensation of the elements. Geochim. Cosmochim. Acta 31, 1215-1238.

Larimer, J. W. 1971. Composition of the Earth: Chondritic or achondritic. Geochim. Cosmochim. Acta 35, 769-786.

Larimer, J. W., Anders, E. 1967. Chemical fractionations in meteorites – II. Abundance patterns and their interpretations. Geochim. Cosmochim. Acta 31, 1239-1270.

Lewis, J. S., Prinn, R. G. 1984. Planets and Their Atmospheres: Origin and Evolution. Academic Press, NY.

Lewis, G. N., Randall, M. 1961. Thermodynamics. (Pitzer, K. S., Brewer, L., eds.) McGraw-Hill, New York, 723 pp.

Lingner, D. W., Huston, T. J., Hutson, M., Lipschutz, M. E. 1987. Chemical studies of H chondrites. I. Mobile trace elements and gas retention ages. Geochim. Cosmochim. Acta 51, 727-739.

Lipschutz, M. E., Woolum, D. S. 1988. Highly labile elements. *In*: Meteorites and the Early Solar System (Kerridge, J. F., Matthews, M. S., eds.) Univ. AZ Press: Tuscon, AZ, pp. 462 – 487.

Lodders, K. 2000. An oxygen isotope mixing model for the accretion and composition of rocky planets. Space Sci. Rev. 92, 341-354.

Lodders, K. 2003. Solar system abundances and condensation temperatures of the elements. Astrophys. J. 591, 1220-1247.

Lodders, K., Fegley, B., Jr. 1997. An oxygen isotope model for the composition of Mars. Icarus 126, 373-394.

Lodders, K., Palme, H., Gail, H.-P. 2009. Abundances of the elements in the solar system. Landolt-Börnstein, New Series, Astronomy and Astrophysics, Springer Verlag, Berlin. submitted.

Luck, J. M., Othman, D. B., Barrat, J. A., Albarede, F. 2003. Coupled ^{63}Cu and ^{16}O excesses in chondrites. Geochim. Cosmochim. Acta 67, 143-151.

Luck, J. M., Othman, D. B., Albarede, F. 2005. Zn and Cu isotopic variations in chondrites and iron meteorites: Early solar nebula reservoirs and parent-body processes. Geochim. Cosmochim. Acta 69, 5351 – 5363.

McSween, Jr., H. Y., Sears, D. W. G., Dodd, R. T. 1988. Thermal metamorphism. *In*: Meteorites and the Early Solar System. (Kerridge, J. F., Matthews, M. S., eds.) Univ. AZ Press: Tucson, 102 – 113.

Morgan, J. W., Janssens, M.-J., Takahashi, H., Hertogen, J., Anders, E. 1985. H-chondrites: trace element clues to their origin. Geochim. Cosmochim. Acta 49, 247-259.

Neal, C. W., Dodd, R. T., Jarosewich, E., Lipschutz, M. E. 1981. Chemical studies of L-chondrites. I. A study of possible chemical sub-groups. Geochim. Cosmochim. Acta 45, 891-898.

Okamoto, H. 1990. The Fe-Tl (iron-thallium) system. Bull. Alloy Phase Diag. 11, 581 – 582.

Otting, W., Zähringer, J. 1967. Total carbon content and primordial rare gases in chondrites. Geochim. Cosmochim. Acta 31, 1949 – 1960.

Raghavan, V. 2008. Fe-Pb-Sb (Iron-Lead-Antimony). J. Phase Equil. Diff. 29, 451.

Rambaldi, E. R., Cendales, M., Thacker, R. 1978. Trace element distribution between magnetic and non-magnetic portions of ordinary chondrites. Earth Planet. Sci. Lett. 40, 175-186.

Schaefer, L., Fegley, B., Jr. 2007a. Outgassing of ordinary chondritic material and some of its implications for the chemistry of asteroids, planets, and satellites. Icarus 186, 462-483.

Schaefer, L., Fegley, B., Jr. 2007b. Trace element chemistry during metamorphism on ordinary chondrite parent bodies. Lunar Planet. Sci. XXXVIII, abstract no. 2280.

Schönbächler, M., Carlson, R. W., Horan, M. F., Mock, T. D., Hauri, E. H. 2008. Silver isotope variations in chondrites: Volatile depletion and the initial ^{107}Pd abundance of the solar system. Geochim. Cosmochim. Acta 72, 5330-5341.

Sears, D. W. G., Weeks, K. S. 1986. Chemical and physical studies of type 3 chondrites – VI: Siderophile elements in ordinary chondrites. Geochim. Cosmochim. Acta 50, 2815 – 2832.

Smales, A. A., Mapper, D., Morgan, J. W., Webster, R. K., Wood, A. J. 1958. Some geochemical determinations using radioactive and stable isotopes. Proc. Second U.N. Conf. Peaceful Uses Atomic Energy, Geneva 2, 242-248.

Spear, F. S. 1995. Metamorphic phase equilibria and pressure-temperature-time paths. Washington, D.C., Mineralogical Society of America, 799 p.

Stolper, E. 1982. Crystallization sequences of calcium-aluminum-rich inclusions from Allende: an experimental study. Geochim. Cosmochim. Acta 46, 2159-2180.

Tandon, S. N., Wasson, J. T. 1968. Gallium, germanium, indium and iridium variations in a suite of L-group chondrites. Geochim. Cosmochim. Acta 32, 1087 – 1109.

Unruh, D. M. 1982. The U-Th-Pb age of equilibrated L chondrites and a solution to the excess radiogenic Pb problem in chondrites. Earth Planet. Sci. Lett. 58, 75-94.

Van Zeggern, F., Storey, S. H. 1970. The computation of chemical equilibria. Cambridge University Press.

Wai, C. M., Wasson, J. T. 1977. Nebular condensation of moderately volatile elements and their abundances in ordinary chondrites. Earth Planet. Sci. Lett. 36, 1-13.

Wai, C. M., Wasson, J. T. 1979. Nebular condensation of Ga, Ge, and Sb and the chemical classification of iron meteorites. Nature 282, 790-793.

Walsh, T. M., Lipschutz, M. E. 1982. Chemical studies of L chondrites. II. Shock-induced trace element mobilization. Geochim. Cosmochim. Acta 46, 2491-2500.

Wang, M.-S., Wolf, S. F., Lipschutz, M. E. 1999. Chemical studies of H chondrites. 10. Contents of thermally labile trace elements are unaffected by late heating. Met. Planet. Sci. 34, 713-716.

Wänke, H. 1981. Constitution of the terrestrial planets. Phil. Trans. R. Soc. London A303, 287-302.

Wieler, R., Günther, D., Hattendorf, B., Pettke, T., Zolensky, M. E. 2000. Chemical composition of halite from the Monahans chondrite determined by laser ablation ICP-MS. Lunar Planet Sci. 31, abstract 1560.

Wodniecki, P., Wodniecka, B., Kulinska, A., Lieb, K. P., Neubauer, M., Uhrmacher, M. 1999. Indium solubility in iron studied with perturbed angular correlations. Hyperfine Int. 120/121, 433-437.

Wolf, S. F., Lipschutz, M. E. 1995. Chemical studies of H chondrites. 4: New data and comparison of Antarctic suites. J. Geophys. Res. 100, 3297-3316.

Wolf, S. F., Lipschutz, M. E. 1998. Chemical studies of H chondrites. 9: Volatile trace element composition and petrographic classification of equilibrated H chondrites. Met. Planet. Sci. 33, 303-312.

Wolf, S. F., Wang, M.-S., Dodd, R. T., Lipschutz, M. E. 1997. Chemical studies of H chondrites. 8. On contemporary meteoroid streams. J. Geophys. Res. 102, 9273-9288.

Wombacher, F., Rehkämper, M., Mezger, K., Münker, C. 2003. Stable isotope compositions of cadmium in geological materials and meteorites determined by multiple-collector ICPMS. Geochim. Cosmochim. Acta 67, 4639-4654.

Wombacher, F., Rehkämper, M., Mezger, K., Bischoff, A., Münker, C. 2008. Cadmium stable isotope cosmochemistry. Geochim. Cosmochim. Acta 72, 646-667.

Wriedt, H. A., Morrison, W. B., Cole, W. E. 1973. Solubility of silver in γ-Fe. Metall. Trans. 4, 1453-1456.

Table 1. H-chondrite trace element abundances

Element[a]	Range	Arithmetic Mean ± 1σ	Geometric Mean	Median	No. of analyses
moderately volatile elements					
As (μg/g)	0.35 – 6.71	2.63 ± 1.20	2.44	2.18	57
Au (ng/g)	116 - 440	222 ± 51.7	217	217	101
Cu (μg/g)	48 - 137	98 ± 21	96.0	98.0	46
Ag (ng/g)	4.69 - 1870	79.9 ± 187	43.5	34.3	117
Sb (ng/g)	1.5 - 480	94.0 ± 75.6	78.1	71.0	119
Ga (μg/g)	3.6 - 11	6.01 ± 1.07	5.93	5.80	121
Ge (μg/g)	5.04 - 16	9.68 ± 3.48	9.08	10.0	19
Rb (μg/g)	0.43 - 4.0	2.21 ± 0.73	2.09	2.17	132
Cs (ng/g)	1.29 - 556	67.8 ± 69.8	39.5	56.9	124
Bi (ng/g)	0.14 - 76.8	7.88 ± 16.7	2.81	2.32	124
Pb (μg/g)	0.031 - 0.66	0.16 ± 0.17	0.10	0.14	13
Zn (μg/g)	4.6 – 144	47.6 ± 16.7	44.8	46.0	137
Te (ng/g)	17 - 3200	382 ± 298	330.	356	107
Sn (μg/g)	--	--	--	0.17	2
Se (μg/g)	4.32 - 20.6	8.26 ± 1.32	8.15	8.20	140
highly volatile elements					
Cd (ng/g)	0.15 - 1240	37.5 ± 159	5.03	4.17	103
Br (μg/g)	0.017 - 1.30	0.34 ± 0.35	0.18	0.20	17
In (ng/g)	0.05 - 103	2.47 ± 11.4	0.53	0.43	107
I (ng/g)	--	--	--	60	1
Tl (ng/g)	0.069 - 220	6.98 ± 26.6	0.97	0.75	95

[a](μg/g) = micrograms per gram (10^{-6} g/g), (ng/g) = nanograms per gram (10^{-9} g/g)

Table 2. L-chondrite trace element abundances

Element[a]	Range	Arithmetic Mean±1σ	Geometric Mean	Median	No. of analyses
moderately volatile elements					
As (μg/g)	0.32 - 4.2	1.42 ± 0.70	1.29	1.35	43
Au (ng/g)	27.9 - 339	162 ± 40.4	156	160	113
Cu (μg/g)	64 - 132	97.9 ± 17.7	96.3	94.7	72
Ag (ng/g)	14.4 - 1258	127 ± 217	75.6	65.0	80
Sb (ng/g)	27.4 - 840	105 ± 108	84.9	76.8	70
Ga (μg/g)	2.8 - 9	5.43 ± 0.84	5.37	5.48	133
Ge (μg/g)	8.9 - 13.4	11.0 ± 1.23	11.1	10.9	18
Rb (μg/g)	0.58 - 7.20	2.49 ± 0.84	2.37	2.32	98
Cs (ng/g)	1.64 - 2270	80.5 ± 258	17.8	13.0	90
Bi (ng/g)	0.09 - 519	17.4 ± 63.5	3.75	3.54	82
Pb (μg/g)	0.022 - 0.56	0.16 ± 0.17	0.063	0.053	6
Zn (μg/g)	17.3 - 291	57.4 ± 29.8	53.1	52.0	117
Te (ng/g)	153 - 1534	404 ± 189	377	376	83
Sn (μg/g)	0.18 - 1.16	0.56 ± 0.39	0.46	0.51	5
Se (μg/g)	3.5 - 13.4	9.21 ± 1.73	9.04	9.30	90
highly volatile elements					
Cd (ng/g)	0.4 - 875	60.1 ± 122	21.7	25.9	65
Br (μg/g)	0.04 - 5.57	0.91 ± 0.99	0.56	0.70	39
In (ng/g)	0.03 - 55	3.37 ± 8.46	0.63	0.50	90
I (μg/g)	0.024 – 5	1.69 ± 2.87	0.16	0.032	3
Tl (ng/g)	0.03 - 119	2.71 ± 3.92	1.19	1.37	77

[a](μg/g) = micrograms per gram (10^{-6} g/g), (ng/g) = nanograms per gram (10^{-9} g/g)

Table 3. LL-chondrite trace element abundances

Element[a]	Range	Arithmetic Mean±1σ	Geometric Mean	Median	No. of analyses
moderately volatile elements					
As (μg/g)	0.08 - 2	1.23 ± 0.39	1.12	1.30	32
Au (ng/g)	97.5 - 306	142 ± 37.5	138	141	49
Cu (μg/g)	60 - 147	94.8 ± 32.9	91.0	86.0	32
Ag (ng/g)	12.3 - 356	79.1 ± 64.1	63.2	62.4	32
Sb (ng/g)	34.5 - 120	73.1 ± 24.2	69.3	67.0	31
Ga (μg/g)	3.3 - 8	5.15 ± 1.02	5.05	5.10	55
Ge (μg/g)	0.2 - 11.2	8.14 ± 4.50	4.61	9.70	5
Rb (μg/g)	0.1 - 5.5	2.13 ± 1.27	1.66	1.90	34
Cs (ng/g)	1.43 - 3070	219 ± 523	96.5	118	33
Bi (ng/g)	0.57 - 66	16.5 ± 16.2	44	11.3	46
Pb (μg/g)	0.058 - 0.35	0.16 ± 0.17	0.11	0.058	3
Zn (μg/g)	28 - 102	54.5 ± 13.8	52.9	53.1	61
Te (ng/g)	96 - 4300	827 ± 975	525	446	32
Sn (μg/g)	--	--	--	0.33	1
Se (μg/g)	4.1 - 18.4	8.62 ± 2.66	8.25	8.50	50
highly volatile elements					
Cd (ng/g)	0.62 - 1248	76.2 ± 235	12.0	17.0	29
Br (μg/g)	0.2 - 1.98	0.69 ± 0.57	0.52	0.50	17
In (ng/g)	0.09 - 81	9.22 ± 17.9	2.43	3.65	38
I (ng/g)	--	--	--	--	0
Tl (ng/g)	0.07 - 114	12.7 ± 25.0	2.16	1.40	42

[a](μg/g) = micrograms per gram (10^{-6} g/g), (ng/g) = nanograms per gram (10^{-9} g/g)

Table 4. Formation temperatures of moderately and highly volatile elements.

		average H-chondrite							
		$P_T = 10^{-4}$ bar				$P_T = 1$ bar			
		pure phases		solid solutions[a]		pure phases		solid solutions[a]	
El	50% T_c[b]	50% T_f	initial solid	50% T_f	host phase[c]	50% T_f	initial solid	50% T_f	host phase[c]
moderately volatile elements									
As	1061	445	As	1359	m	582	As	2202	m
Au	1061	924	Au	1500	m	1200	Au	2572	m
Cu	1033	1338	Cu_2S	1768	m	1952	Cu_2S	2839	m
Ag	992	875	Ag	1471	m	1148	Ag	2691	m
Sb	976	574	Sb	1458	m	736	Sb	2623	m
Ga	971	902	Ga_2O_3	1313	m	1111	Ga_2O_3	2670	m
Ge	885	619	Ge	895	m	852	Ge	1765	m
Rb	798	675	RbCl	740	p	911	RbCl	971	p
Cs	797	566	CsI	640	p	742	CsI	836	p
Bi	743	548	Bi	1253	m	711	Bi	2355	m
Pb	724	635	PbSe	1215	m	772	PbSe	2355	m
Zn	723	840	$ZnCr_2O_4$	1119	s	1155	ZnS	1716	s
Te	705	572	$FeTe_{0.9}$	1228	s	757	$FeTe_{0.9}$	1962	s
Sn	703	576	SnS	1142	m	828	Sn	2300	m
Se	688	626	ZnSe	1463	s	875	ZnSe	2302	s
highly volatile elements									
Cd	650	547	CdTe	798	s	718	CdTe	1406	s
Br	544	632	RbBr	828	s	843	RbBr	1397	s
In	535	423	InS	1465	m	492	InS	2605	m
I	533	566	CsI	786	s	742	CsI	1351	s
Tl	531	375	TlI	1112	m	475	TlI	2225	m

[a]ideal solid solutions. [b]condensation temperatures in the solar nebula at 10^{-4} bar taken from Lodders (2003). [c]host phases: m – metal, s – sulfide, p – plagioclase.

Table 5. Volatility Sequences in Ordinary Chondritic Material

	Increasing volatility→
H @ 1 bar[a]	Cu, Au, Zn, Ag, Ga, Rb, Se, Ge, Br, Sn, Pb, Te, Cs, I, Sb, Cd, Bi, As, In, Tl
	Cu, Ag, Ga, Sb, In, Au, Bi, Pb, Se, Sn, Tl, As, Te, Ge, Zn, Cd, Br, I, Rb, Cs
H @ 10^{-4} bar[a]	Cu, Au, Ga, Ag, Zn, Rb, Pb, Br, Se, Ge, Sn, Sb, Te, Cs, I, Bi, Cd, As, In, Tl
	Cu, Au, Ag, In, Se, Sb, As, Ga, Bi, Te, Pb, Sn, Tl, Zn, Ge, Br, Cd, I, Rb, Cs
Solar[b]	As, Au, Cu, Ag, Sb, Ga, Ge, Rb, Cs, Bi, Pb, Zn, Te, Sn, Se, Cd, Br, In, I, Tl
Mobility[c]	Ga, Se, Cs, Zn, Ag, In, Te, Tl, Bi

[a]pure phases, *ideal solid solutions*. [b]Lodders (2003) [c]Tieschitz (H/L3.6) – Ikramuddin et al. (1977).

Figure Captions

Figure 1. Abundances of trace elements in H- (top), L- (middle), and LL- chondrite (bottom) falls, relative to CI chondrites. The abundances are expressed in terms of the geometric means; lines represent the standard error on the geometric means.

Figure 2. (a) Abundances of In, Tl, and Bi as a function of petrographic type in H3 and H/L3 chondrites. Solid dots are H3 chondrites, hollow dots are H/L3 chondrites. (b) Abundances of In and Tl as a function of petrographic type in LL3 chondrites.

Figure 3. 50% formation temperatures (T_f) of As, Ag, Au, Bi, Cu, Ga, Ge, Fe, In, Pb, Sb, Sn, and Tl as a function of pressure. Trace elements are found (a) as pure phases, and (b) ideal solid solutions with metal (Ag, As, Au, Bi, Cu, Fe, Ga, Ge, In, Pb, Sb, Sn, Tl) and sulfide (InS, PbS, Tl_2S). Abundances are for average H-chondritic material. The P-T profile of the asteroid *6 Hebe* calculated by Schaefer and Fegley (2007a) is shown as a dotted line. The shaded region denotes a range of melting temperatures for ordinary chondrites.

Figure 4. 50% formation temperatures (T_f) of Cd, S, Se, Te, and Zn as a function of pressure. Trace elements are found (a) as pure phases, and (b) ideal solid solutions with sulfides (Ag_2S, CdS, Bi_2S_3, FeS, $FeSe_{0.961}$, ZnS), metal (Cd), and silicates (Zn-silicates). Abundances are for average H-chondritic material. The P-T profile of the asteroid *6 Hebe* calculated by Schaefer and Fegley (2007a) is shown as a dotted line. The shaded region denotes a range of melting temperatures for ordinary chondrites.

Figure 5. 50% formation temperatures (T_f) of Br, Cs, I, and Rb as a function of pressure. Trace elements are found (a) as pure phases, and (b) ideal solid solutions with plagioclase (Cs, Rb) and sulfide ($FeBr_2$, FeI_2). Abundances are for average H-chondritic material. The P-T profile of the

asteroid *6 Hebe* calculated by Schaefer and Fegley (2007a) is shown as a dotted line. The shaded region denotes a range of melting temperatures for ordinary chondrites.

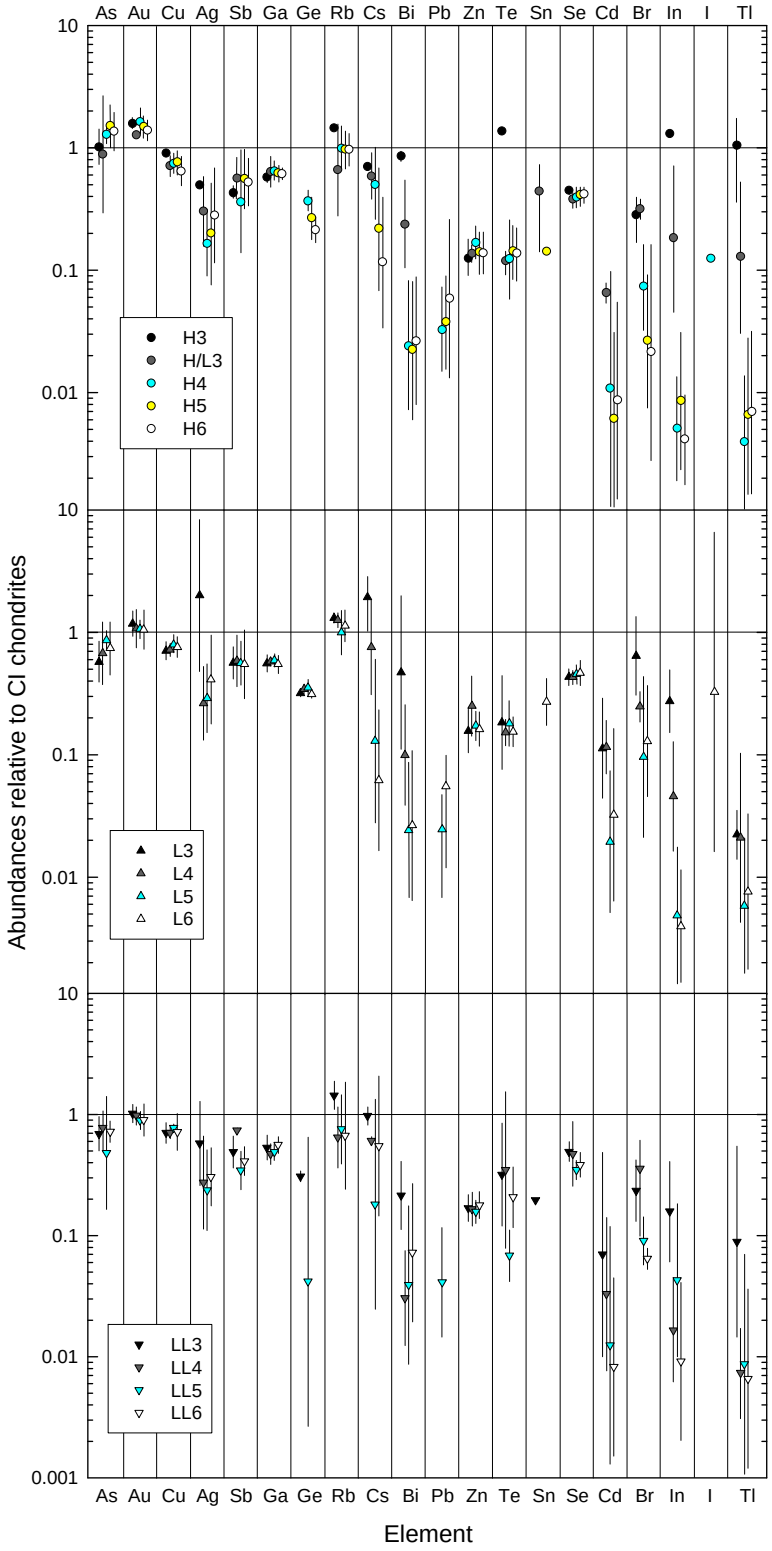
As Au Cu Ag Sb Ga Ge Rb Cs Bi Pb Zn Te Sn Se Cd Br In I Tl
10
1
0.1
0.01
H3
H/L3
H4
H5
H6
L3
L4
L5
L6
LL3
LL4
LL5
LL6
0.001
Abundances relative to CI chondrites
Element

Figure 1.

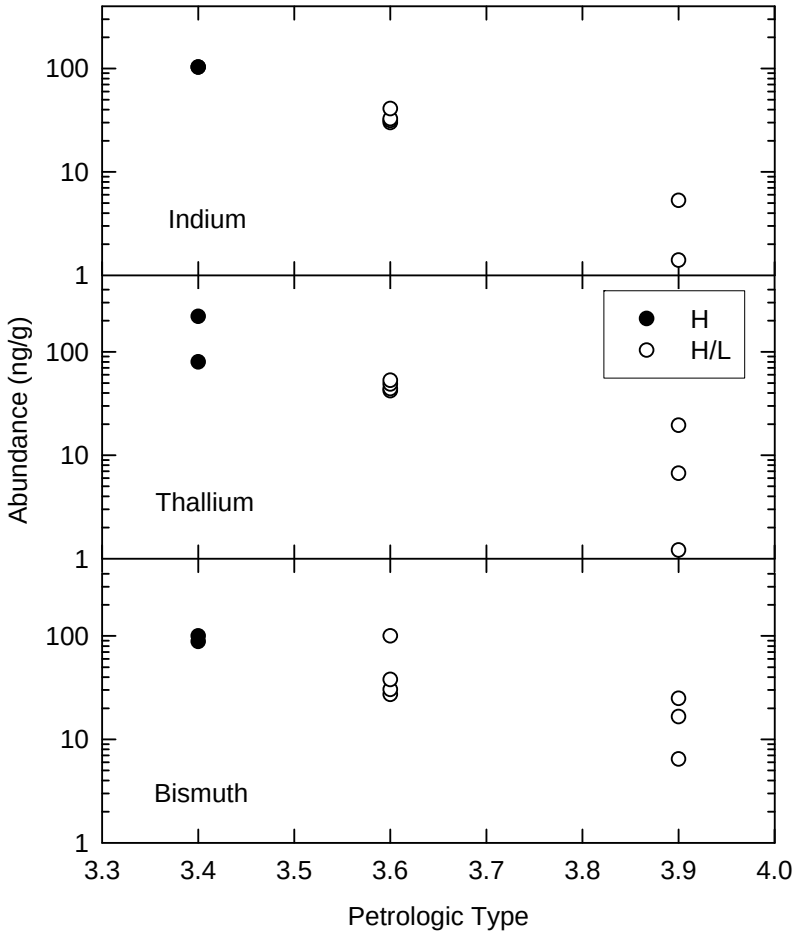

Figure 2a. In, Bi, Tl in type H3 and H/L3 chondrites

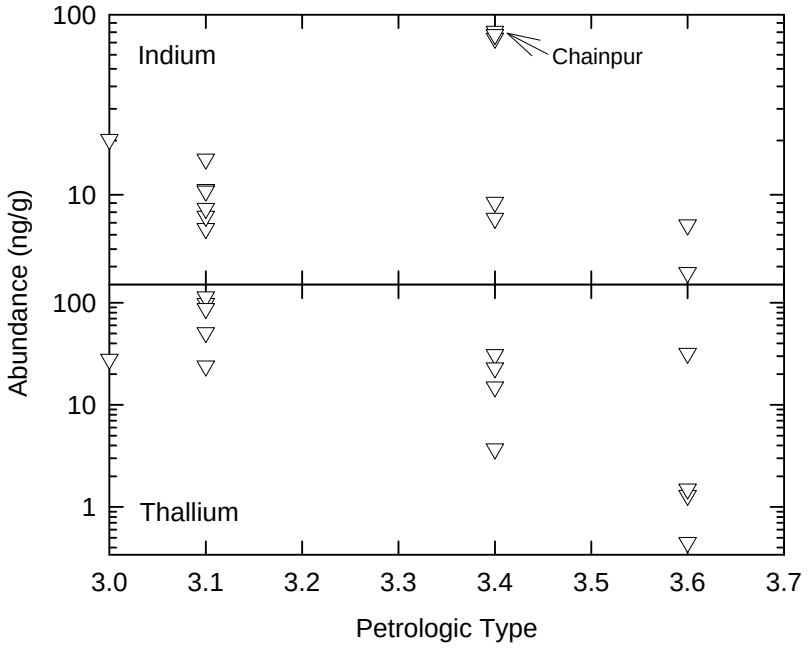

Fig. 2b, In and Tl in LL3 chondrites

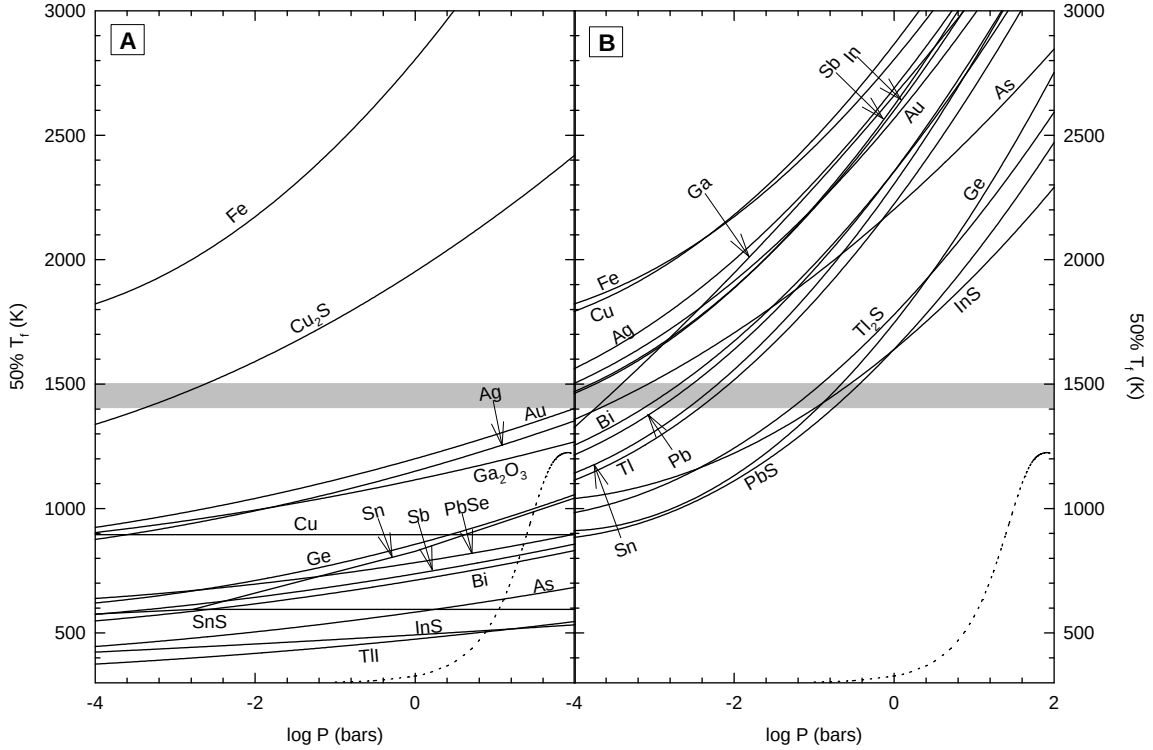

Fig. 3. Metal solid solution

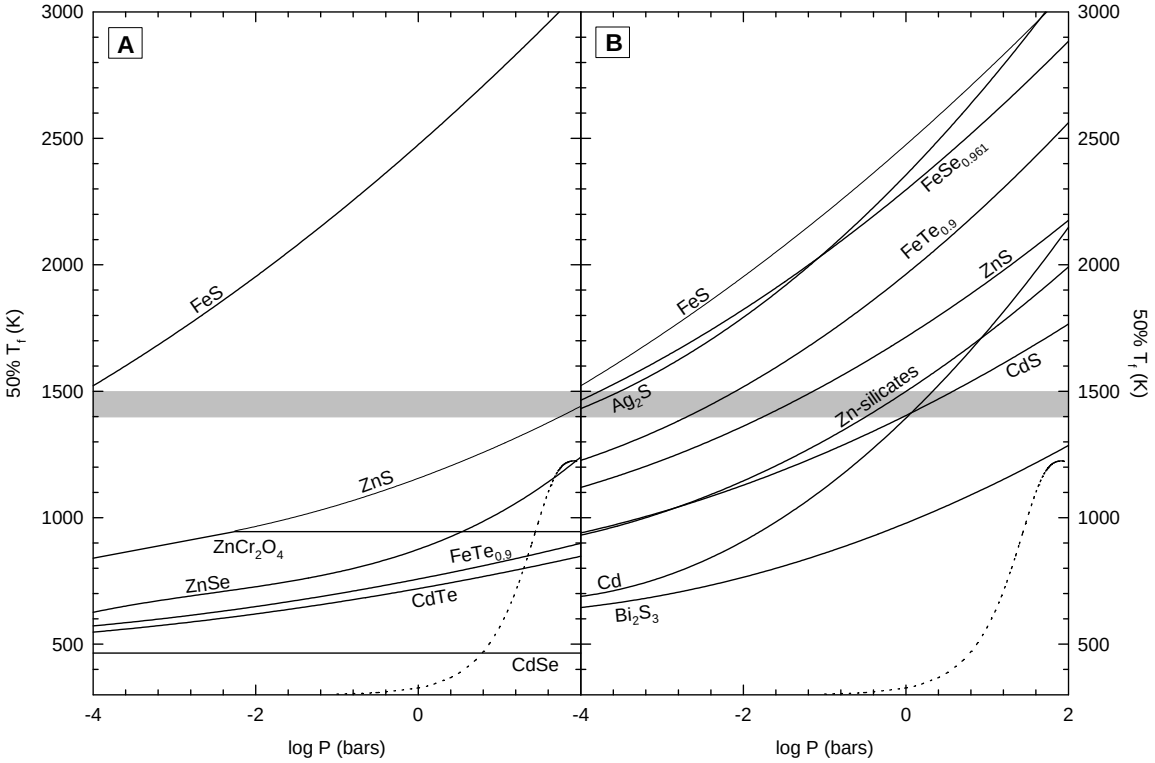

Fig. 4. Sulfide Solid Solution

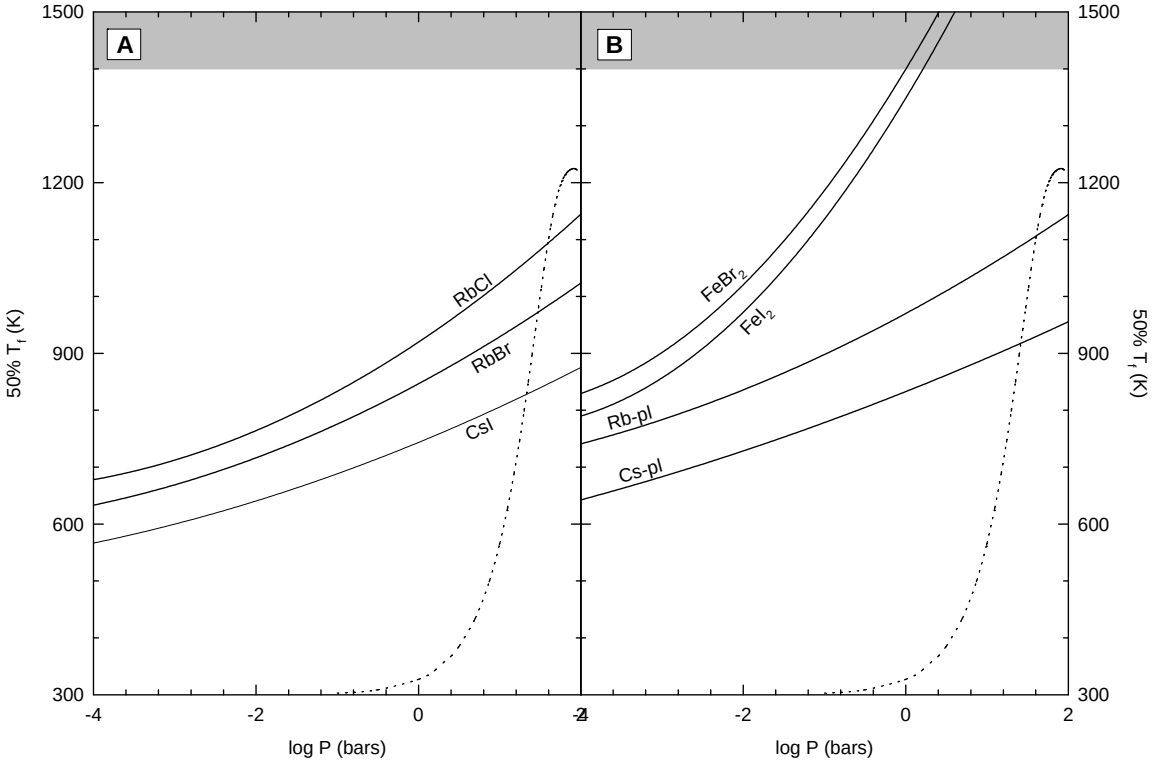

Fig. 5. Plagioclase Solid Solution